Molecular Microbiology (2017) 104(4), 553–567 ■
doi:10.1111/mmi.13645
First published online 2 March 2017

The TORC1–Sch9–Rim15 signaling pathway represses yeast-to-hypha transition in response to glycerol availability in the oleaginous yeast *Yarrowia lipolytica*

Shu-Heng Liang,[1] Heng Wu,[1] Rui-Rui Wang,[1] Qiang Wang,[1] Tao Shu[1] and Xiang-Dong Gao [1,2]*

[1]*Hubei Key Laboratory of Cell Homeostasis, College of Life Sciences, Wuhan University, Wuhan, China.*
[2]*Hubei Provincial Cooperative Innovation Center of Industrial Fermentation, Wuhan, China.*

Summary

The yeast-to-hypha dimorphic transition is important for survival under nutrient starvation in fungi. The oleaginous yeast *Yarrowia lipolytica* grows in the oval-shaped yeast form in glycerol media whereas it adopts a filamentous form in glucose media. It is not clear why this yeast responds differently to glycerol and glucose. Here, we show that glycerol blocks dimorphic transition even in the presence of glucose whereas glycerol depletion induces filamentous growth, suggesting that dimorphic transition is repressed in response to glycerol availability. We show that the repression of dimorphic transition in glycerol media is mediated by the TORC1–Sch9 signaling pathway as both TORC1 inhibition and the loss of YlSch9 cause hyperfilamentation. TORC1–Sch9 signaling inhibits the nuclear translocation of YlRim15, a protein kinase that positively regulates filamentous growth, preventing it from entering the nucleus to activate the transcription of genes implicated in filamentous growth. Interestingly, TORC1–Sch9 signaling appears not to inhibit YlRim15 in glucose media, which could explain why *Y. lipolytica* responds differently to glycerol and glucose. We identified *MHY1*, a transcription factor-encoding gene known to be critical for filamentous growth, as one target regulated by the TORC1–Sch9–Rim15 signaling pathway. Our results provide new insights in the regulation of dimorphic transition in yeast.

Accepted 7 February, 2017. *For correspondence. E-mail xdgao@whu.edu.cn; Tel. (+86) 15327283490.

Introduction

Some fungal species can grow either in the ovoid yeast form or in the filamentous form (hyphae or pseudohyphae). The yeast-to-hypha dimorphic transition can be induced by environmental factors such as temperature, pH and the accessibility of nitrogen source (Lengeler *et al*., 2000; Berman and Sudbery, 2002; Palecek *et al*., 2002). Dimorphic transition is thought to be a foraging behavior through which fungal cells can spread out and approach distant nutrients (Gimeno *et al*., 1992). It is important for cell survival in response to environmental changes and is an important virulence factor for some pathogenic fungi including the human pathogen *Candida albicans* (Lengeler *et al*., 2000; Berman and Sudbery, 2002; Palecek *et al*., 2002; Kadosh, 2013; Lu *et al*., 2014)

Studies in two yeast species *Saccharomyces cerevisiae* and *C. albicans* showed that the two Ras-controlled signaling pathways – Kss1/Cek1 mitogen-activated protein kinase (MAPK) pathway and the cAMP-protein kinase A (PKA) pathway play important, positive roles in the control of dimorphic transition (Mosch *et al*., 1996; Csank *et al*., 1998; Robertson and Fink, 1998; Leberer *et al*., 2001). In contrast to these pathways that operate under nutrient-poor conditions, the signaling pathway that represses dimorphic transition under nutrient-rich condition is poorly understood.

Yarrowia lipolytica is a dimorphic yeast species distantly related to *S. cerevisiae* and *C. albicans* (Dujon *et al*., 2004; Groenewald *et al*., 2014). Unlike the latter two yeast species, *Y. lipolytica* can utilize *n*-alkanes, fatty acids and vegetable oils as the sole carbon sources (Barth and Gaillardin, 1997; Zinjarde *et al*., 2008). When cultivated in vegetable oils, *Y. lipolytica* grows in the oval-shaped yeast form (Zinjarde *et al*., 2008). However, the cells become elongated and form pseudohyphae or hyphae when cultivated in glucose media (Ruiz-Herrera and Sentandreu, 2002). It is not understood the molecular mechanism underlying this morphological change. A previous study in *C. albicans* showed that TORC1–Sch9 signaling represses dimorphic transition

under hypoxia at high CO_2 levels (Stichternoth *et al.*, 2011). This observation led us to investigate the role of TORC1–Sch9 signaling in the control of dimorphic transition in different carbon sources.

TOR is a conserved Ser/Thr protein kinase that regulates cell growth and metabolism in eukaryotes in response to environmental cues (Wullschleger *et al.*, 2006). TOR exists in two structurally and functionally distinct protein complexes – TOR complex 1 (TORC1) and TOR complex 2 (TORC2). Under favorable conditions, TORC1 is active and promotes robust translation initiation, nutrient import and ribosome biogenesis but represses starvation- and stress-associated processes, such as stress response, the utilization of nonpreferred nutrients and autophagy in *S. cerevisiae* and mammals (Thomas and Hall, 1997; Schmelzle and Hall, 2000; Rohde *et al.*, 2001). TORC1 in the filamentous fungus *Fusarium oxysporum* regulates nitrogen utilization (López-Berges *et al.*, 2010). In the fission yeast *Schizosaccharomyces pombe*, TORC1 also represses sexual development during vegetative growth (Matsuo *et al.*, 2007). The previous report that TORC1 represses dimorphic transition in *C. albicans* has further expanded the repertoire of cellular functions that TORC1 negatively regulates. In contrast to TORC1, TORC2 regulates cell wall integrity, receptor endocytosis and actin cytoskeleton polarization as shown in *S. cerevisiae* (Schmidt *et al.*, 1996; deHart *et al.*, 2003).

In *S. cerevisiae*, TORC1 functions in the repression of stress response via the protein kinase Sch9 (Fabrizio *et al.*, 2001; Urban *et al.*, 2007), the yeast ortholog of mammalian S6K1. When nutrient is abundant, Sch9 is activated by TORC1 by phosphorylation at the hydrophobic motif (Urban *et al.*, 2007). Sch9 activation also requires the phosphorylation at the activation loop by Pkh1 (PDK1 in mammals). Activated Sch9 inhibits the nuclear translocation of the protein kinase Rim15 (Pedruzzi *et al.*, 2003; Mirisola *et al.*, 2014). When nutrient is limited, TORC1 and Sch9 activities are low. Rim15 is dephosphorylated, which leads to its activation and translocation to the nucleus (Pedruzzi *et al.*, 2003). Activated Rim15 in the nucleus stimulates the transcription factors Msn2/4 and Gis1 to activate stress-responsive element (STRE)-gene expression and post-diauxic shift (PDS)-driven gene expression, respectively (Martinez-Pastor *et al.*, 1996; Pedruzzi *et al.*, 2000). In contrast to the TORC1–Sch9 signaling in the repression of stress response, the downstream target of TORC1–Sch9 in the repression of dimorphic transition is not known.

Here, we show that the TORC1–Sch9 signaling pathway represses dimorphic transition in *Y. lipolytica* in the presence of glycerol, a preferred carbon source for this yeast species. More importantly, we identify the *Y. lipolytica* homolog of Rim15 to be the major downstream effector of TORC1–Sch9 in the repression of dimorphic transition. Interestingly, TORC1–Sch9 signaling does not appear to inhibit YlRim15 in glucose media, which could explain the morphological difference of cells grown in glycerol and glucose media. These findings provide new insight in the understanding of how dimorphic transition is regulated in response to different carbon sources.

Results

Dimorphic transition is repressed in glycerol but not in glucose media in Y. lipolytica

Y. lipolytica can use either glucose or glycerol as the sole carbon source to grow. However, cells exhibited different morphology in glycerol and glucose media. Cells grown in liquid synthetic glycerol medium (YNBG) were uniformly oval-shaped (typical yeast form) (Fig. 1A, top panel). Very few short pseudohyphae (6%, $n = 509$), which comprise mostly three to four oval-shaped cells, could be detected. In contrast, cells grown in liquid glucose medium (YNBD) showed a much more elongated morphology and slightly more cells (10%, $n = 536$) formed short pseudohyphae (Fig. 1A, top panel). Cells grown on YNBD agar also exhibited much longer radial filaments emanating from the colonies than those grown on YNBG agar (Fig. 1A, bottom panel). These results suggest that filamentous differentiation is strong in glucose but very weak in glycerol medium. We observed that cells cultivated in liquid medium or on solid medium containing both glycerol and glucose (YNBGD) displayed morphology identical to that of cells cultivated in glycerol medium (Fig. 1A), indicating that glycerol could repress filamentation induced by glucose.

In contrast, we observed that glycerol depletion induces filamentation as *Y. lipolytica* cells pregrown in liquid YNBG medium exhibited filamentous differentiation after being shifted to YNB agar, which does not contain any carbon source, whereas cells grown on YNBG agar did not filament at similar growth stage (similar amount of cells in the microcolonies) (Fig. 1B). Caffeine is an inhibitor of TORC1 and can induce starvation in the cells (Wanke *et al.*, 2008). We observed that cells grown on YNBG agar supplemented with caffeine also exhibited filamentation (Fig. 1B), indicating that glycerol depletion has an impact similar to starvation. Cells shifted to YNBD agar also displayed filamentation (Fig. 1B), in agreement with the view that glucose does not repress filamentation.

Y. lipolytica cells can also grow vigorously in YNB medium supplemented with fructose or peptone. They can also grow in sodium oleate, sodium lactate and sodium citrate albeit slower. We found that cells grown in liquid YNB medium supplemented with fructose, peptone, sodium lactate or sodium citrate exhibited

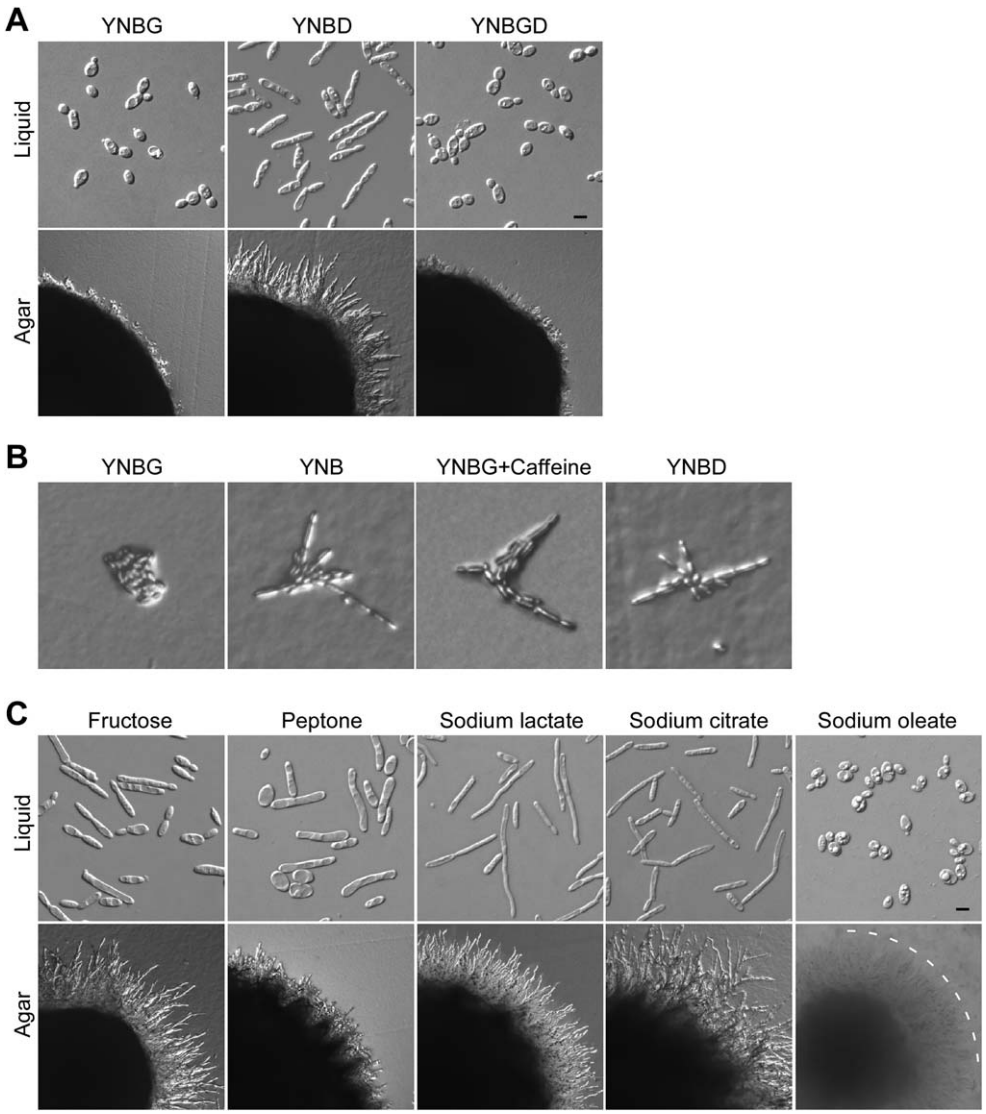

Fig. 1. Morphology of *Y. lipolytica* cells grown in YNB media with different carbon sources.
A. Top panel: cells of wild-type strain PO1a carrying pINA445 were grown in liquid YNBG and YNBGD media for 14 h and in YNBD medium for 16 h. Bottom panel: the same cells were grown for 2 days on YNBG, YNBD and YNBGD agar media. Uracil was supplemented in the media.
B. Cells of strain PO1a carrying pINA445 and pINA443 (*CEN*, YI*URA3*) were pregrown in liquid YNBG medium for 14 h, washed and shifted onto YNBG, YNB, YNBG containing 1 mM caffeine and YNBD agar media. Microcolonies were photographed after growth for 8 h.
C. Top panel: wild-type cells carrying pINA445 were grown in liquid YNB medium supplemented with fructose, peptone, sodium lactate, sodium citrate and sodium oleate for 16, 14, 18, 24 and 18 h, respectively. Bottom panel: cells as shown in (A) were grown on solid agar media for 2, 2, 3, 5 and 3 days, respectively. Uracil was supplemented in the media. The filaments formed by cells grown on solid oleate medium are less clear to visualize due to the less transparency of this particular medium. The leading front of filaments is indicated by white dash line. Scale bars, 5 μm.

elongated morphology and cells grown on solid agar medium displayed strong pseudohyphal outgrowth (Fig. 1C), indicating that filamentous differentiation is induced. Interestingly, cells grown in liquid oleate medium adopted an oval shape similar to that of cells grown in glycerol medium. However, on solid oleate medium, cells displayed strong pseudohyphal outgrowth (Fig. 1C), indicating that, unlike glycerol, oleate does not dramatically repress dimorphic transition on solid medium. These results suggest that the repressive role of glycerol on dimorphic transition appears to be unique.

Together, our results show that *Y. lipolytica* responds to glycerol differently from glucose and other carbon sources with respect to dimorphic transition. Glycerol but not glucose strongly represses dimorphic transition.

The TORC1–Sch9 signaling pathway represses dimorphic transition in response to glycerol but not glucose availability

TORC1 is a master regulator in the control of cell growth in response to nutrient availability (Wullschleger *et al.*, 2006). The TORC1–Sch9 pathway is known to repress dimorphic transition in *C. albicans*, albeit only under hypoxia and high levels of CO_2 (Stichternoth *et al.*, 2011). To investigate whether the TORC1–Sch9 pathway may have mediated the repression of dimorphic transition by glycerol, we wanted to delete the homolog of TOR in *Y. lipolytica*. The ORF YALI0F07084 in the *Y. lipolytica* genome encodes a single homolog of *S. cerevisiae* Tor1 and Tor2. The encoded protein shares the highest degree of amino acid sequence identity (53% overall identity) with *S. cerevisiae* Tor1. The deletion of YALI0F07084g (Yl*TOR1*) in the wild-type strain PO1a did not succeed. YlTor1 may be essential for growth.

Rapamycin and caffeine are known to inhibit TORC1 activity in *S. cerevisiae* and mammals (Sarkaria *et al.*, 1999; Loewith *et al.*, 2002; Reinke *et al.*, 2006; Wanke *et al.*, 2008). We then added rapamycin and caffeine to the glycerol medium and examined the effect of TORC1 inhibition on dimorphic transition. Remarkably, we observed that the addition of rapamycin to YNBG agar at the concentration of 3.4 nM or higher caused hyperfilamentation. Long and thick radial filaments emanated from the colonies (Fig. 2A, left panel). Rapamycin at the concentration between 6.8 and 13.7 nM stimulated strong pseudohyphal outgrowth but did not dramatically reduce growth (indicated by colony size). Caffeine could also induce hyperfilamentation but it requires higher concentration, at about 1.0 mM (Fig. 2A, right panel). This finding suggests that TORC1 negatively regulates dimorphic transition in *Y. lipolytica*. Higher concentration of rapamycin (27.3 nM) or caffeine (5.0 mM) also reduced growth as the colony sizes of treated samples were markedly smaller than that of the untreated control (Fig. 2A).

The *S. cerevisiae* homolog of mammalian S6K kinase, Sch9, is a downstream target of TORC1 and plays multiple roles in TORC1-regulated cell growth, translation, ribosome biogenesis and entry into G_0 phase in *S. cerevisiae* (Kaeberlein *et al.*, 2005; Urban *et al.*, 2007). More importantly, *C. albicans* CaSch9 is known to negatively regulate dimorphic transition, though only under hypoxia with elevated CO_2 levels (Stichternoth *et al.*, 2011). CaSch9 also plays a role in chromosome segregation (Varshney *et al.*, 2015). To investigate whether TORC1 may repress dimorphic transition in *Y. lipolytica* via the homolog of *S. cerevisiae* Sch9, we deleted Yl*SCH9* (YALI0D14542) in the wild-type strain. Successful deletion was confirmed by PCR analysis (data not shown) and Yl*SCH9* complementation (Fig. 2B).

Yl*sch9*Δ cells cultivated in liquid YNBG medium were more elongated than wild-type cells (Fig. 2B). A total of 28% of Yl*sch9*Δ cells ($n = 402$) exhibited an elongated morphology with an average length of 11.8 ± 2.1 μm ($n = 160$) for the mother cells. The rest of cells showed an average length of 6.9 ± 0.6 μm ($n = 174$) for the mother cells, comparable to the average length of 7.0 ± 0.6 μm ($n = 163$) for wild-type mother cells. Yl*sch9*Δ cells also exhibited stronger pseudohyphal outgrowth than wild-type cells on YNBG agar (Fig. 2B), the same growth condition whereby TORC1-inhibited cells exhibited the hyperfilamentous phenotype. These results suggest that, like TORC1, YlSch9 is a negative regulator of filamentous growth. Like wild-type cells, Yl*sch9*Δ cells exhibited filamentation upon glycerol depletion (on YNB agar) and caffeine-induced starvation (Fig. 2C). Remarkably, Yl*sch9*Δ cells also exhibited filamentation under glycerol-rich condition whereas wild-type cells did not (Fig. 2C, see YNBG), indicating that Yl*sch9*Δ cells are derepressed from glycerol repression. YlSch9 may be the player that mediates the repression by glycerol. Consistent with YlSch9's negative role in dimorphic transition, we found that Yl*SCH9* overexpression blocked filamentous growth in wild-type cells on YNBD agar as well as in liquid YNBD and hypha-inducing YNDC7 media (Fig. S1).

Yl*sch9*Δ cells did not exhibit obvious difference in cell morphology compared to wild-type cells when grown in liquid YNBD medium, which uses glucose as the carbon source (Fig. 2B). The average length of mother cells for Yl*sch9*Δ cells was 14.0 ± 1.7 μm ($n = 98$), close to that of wild-type cells (13.8 ± 1.9 μm, $n = 96$). This result indicates that the repressive role of YlSch9 on dimorphic transition is apparent in glycerol but undetectable in glucose media.

The repressive role of YlSch9 is also undetectable in fructose media and sodium oleate media. Yl*sch9*Δ cells grown in liquid fructose medium showed an elongated morphology similar to wild-type cells (Fig. S2A). The average length of the mother cells (15.5 ± 1.4 μm, $n = 80$) is comparable to that of wild-type cells (15.8 ± 1.3 μm, $n = 76$). Yl*sch9*Δ cells grown in liquid sodium oleate medium were still in the oval-shaped yeast form just like wild-type cells (Fig. S2B). On both solid fructose medium and sodium oleate medium, Yl*sch9*Δ cells did not exhibit enhanced pseudohyphal outgrowth compared to wild-type cells (Fig. S2A and B). These results indicate that YlSch9 represses dimorphic transition specifically in glycerol but not in glucose, fructose or sodium oleate media.

The similar hyperfilamentous phenotype between TORC1-inhibited cells and Yl*sch9*Δ cells in glycerol media suggests that YlSch9 may function in the TORC1 pathway. We found that TORC1 represses dimorphic transition mainly via YlSch9 since pseudohyphal

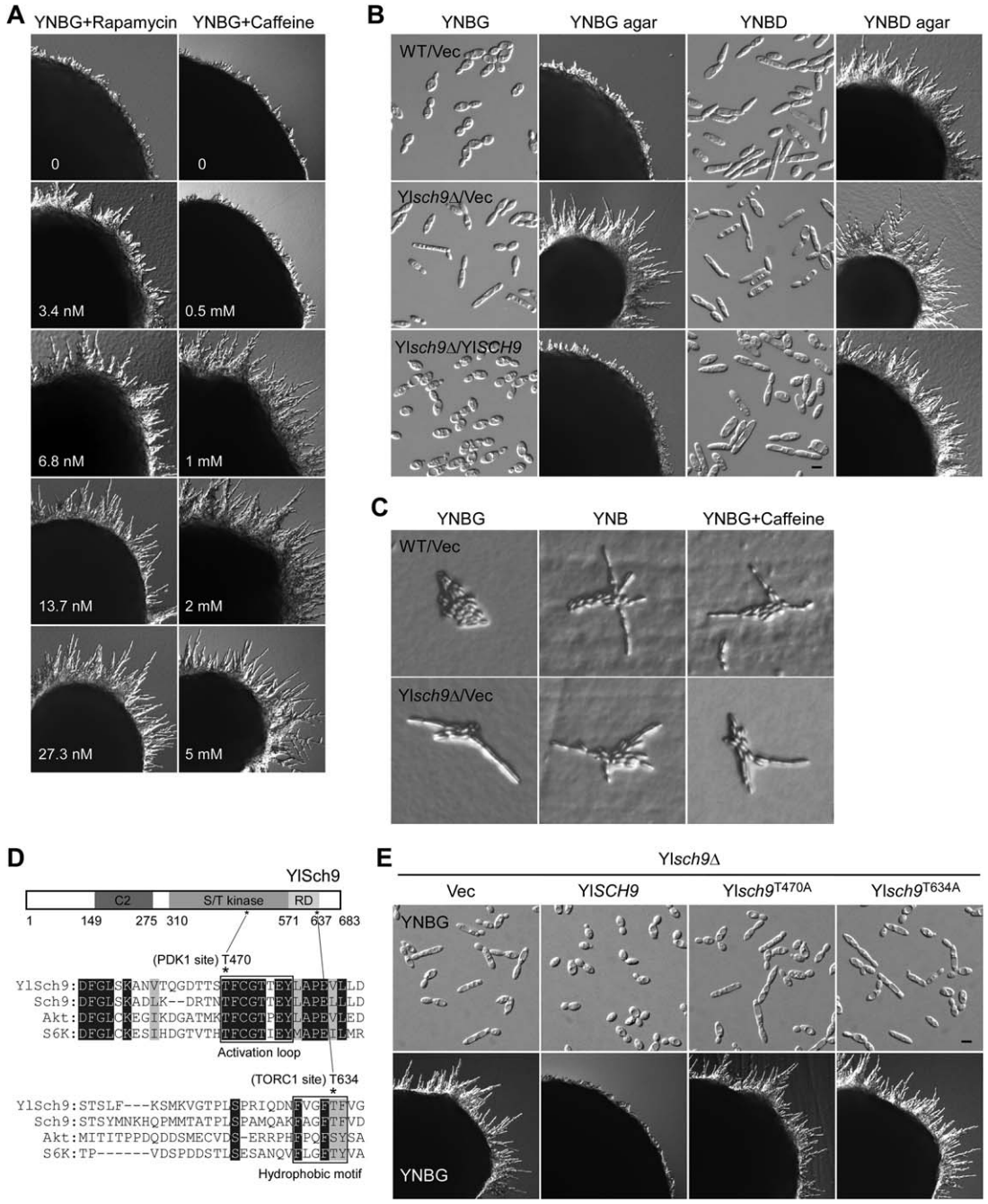

Fig. 2. The TORC1–Sch9 pathway represses dimorphic transition in glycerol medium.
A. TORC1 inhibition causes hyperfilamentation in glycerol medium. Cells of strain PO1a carrying pINA445 were grown on YNBG agar supplemented with uracil and different concentrations of rapamycin or caffeine. Colonies were photographed after 2 days.
B. YI*sch9*Δ cells are hyperfilamentous in glycerol media. Cells of strain PO1a carrying pINA445 (WT/Vec) and cells of YI*sch9*Δ carrying pINA445 (YI*sch9*Δ/Vec) or pINA445-YlSCH9 (YI*sch9*Δ/YI*SCH9*) were grown for 14 h in liquid YNBG or 16 h in YNBD media supplemented with uracil and for 2 days on agar media.
C. Glycerol depletion induces filamentation. Cells of PO1a and YI*sch9*Δ strains carrying pINA445 and pINA443 were pregrown in liquid YNBG medium, washed and shifted onto YNBG, YNB and YNBG containing 1 mM caffeine agar media. Microcolonies were photographed after growth for 8 h.
D. Schematic representation of the domains of YlSch9 and the alignment of sequences at the activation loop and hydrophobic motif (marked in boxes) of YlSch9, *S. cerevisiae* Sch9, human Akt and S6K1. Identical and similar residues are highlighted in black and gray, respectively. RD, regulatory domain.
E. YI*sch9*^{T470A} and YI*sch9*^{T634A} mutants are nonfunctional. Cells of YI*sch9*Δ carrying pINA445 (Vec) or YI*SCH9*, YI*sch9*^{T470A} and YI*sch9*^{T634A} in pINA445 were grown in liquid YNBG medium supplemented with uracil for 14 h or on YNBG agar for 2 days. Scale bars, 5 μm.

outgrowth of Yl*sch9*Δ cells was not stimulated further by rapamycin or caffeine (see later Fig. 3A). *S. cerevisiae* Sch9 and human S6K1 and Akt/PKB require the phosphorylation at two sites for their full activity (Isotani *et al.*, 1999; Mora *et al.*, 2004; Sarbassov *et al.*, 2005; Urban *et al.*, 2007). YlSch9 contains these two conserved threonine residues: T470 in the activation loop that is phosphorylated by PDK1 and T634 in the hydrophobic motif that is phosphorylated by TORC1 (Fig. 2D). We found that the Yl*sch9*^{T634A} mutant, which replaced the TORC1 phosphorylation site T634 by alanine, did not reduce hyperfilamentation of Yl*sch9*Δ cells back to normal (Fig. 2E), indicating that the Yl*sch9*^{T634A} mutant is not functional. Thus, YlSch9 appears to require T634 phosphorylation by TORC1 for activation. The phosphorylation of T470 by PDK1 is also essential for YlSch9 activation as Yl*sch9*^{T470A} mutant did not rescue Yl*sch9*Δ cells either (Fig. 2E). The YlSch9^{T470A} and YlSch9^{T634A} mutants are stably expressed as determined by immunoblotting (Fig. S3).

Apart from a phenotype in filamentation, Yl*sch9*Δ cells showed partial defect in growth as the colonies formed by Yl*sch9*Δ cells were markedly smaller than those formed by wild-type cells on solid glycerol medium and glucose medium (Fig. S4A), suggesting that YlSch9 may regulate growth. This phenotype is similar to *C. albicans* Ca*sch9*Δ/Δ cells grown on YPD medium (Liu *et al.*, 2010; Stichternoth *et al.*, 2011). *C. albicans* Ca*sch9*Δ/Δ cells exhibited resistance to SDS, a plasma membrane-disturbing agent, and sensitivity to high concentrations of salts (Liu *et al.*, 2010; Stichternoth *et al.*, 2011). We found that Yl*sch9*Δ cells were neither resistant nor sensitive to SDS or high concentrations of sodium chloride (Fig. S4B and C), suggesting that YlSch9 may not play a role in cell wall stress response and high osmolarity response.

Taken together, our results show that the TORC1–Sch9 signaling pathway is responsible for the repression of dimorphic transition by glycerol in *Y. lipolytica*. Both TORC1 inhibition and the lack of YlSch9 induce filamentation. This pathway may play a role in integrating glycerol sensing to the repression of filamentous differentiation.

YlRim15 may be the major downstream target of TORC1–Sch9 signaling pathway in the repression of dimorphic transition

Although the repressive role of TORC1–Sch9 signaling on dimorphic transition has been reported previously in *C. albicans* (Stichternoth *et al.*, 2011), the downstream target of the TORC1–Sch9 signaling pathway remains elusive. In *S. cerevisiae*, the protein kinase Rim15 functions downstream of Sch9 in the control of transcriptional reprogramming upon nutrient starvation (Pedruzzi *et al.*, 2003; Roosen *et al.*, 2005; Swinnen *et al.*, 2006). However, it is not known whether Rim15 may control dimorphic transition, let alone whether it may function downstream of Sch9 in this process. We then investigated whether the *Y. lipolytica* homolog of Rim15 may function as the downstream target of YlSch9 in dimorphic transition. The *Y. lipolytica* genome encodes a single homolog of *S. cerevisiae* Rim15 – YALI0F14707. It shares the highest degree of amino acid sequence identity (67%) with Rim15 and contains the signature PAS, C_2HC zinc finger, protein kinase and REC domains (see later Fig. 4B). We named it YlRim15. We deleted Yl*RIM15* in the wild-type and Yl*sch9*Δ strains and examined the phenotype of deletion mutants. Successful deletion of Yl*RIM15* was confirmed by PCR analysis (data not shown) and Yl*RIM15* complementation (Fig. 3B, also later Fig. 4D).

Yl*rim15*Δ cells cultivated in liquid YNBG medium did not differ in morphology from wild-type cells (Fig. 3A, top row). However, Yl*rim15*Δ cells exhibited weaker pseudohyphal outgrowth on YNBG agar than wild-type cells (Fig. 3A, second row), suggesting that YlRim15 may positively regulate dimorphic transition. We observed that pseudohyphal outgrowth of Yl*rim15*Δ cells grown on YNBG agar could be slightly stimulated by rapamycin or caffeine. However, no massive long radial filaments were induced by TORC1 inhibitors as wild-type cells did (Fig. 3A, lower two rows), indicating that the hyperfilamentation of TORC1-inhibited cells largely depends on YlRim15. YlRim15 may act downstream of TORC1 in the control of dimorphic transition.

We then investigated whether YlRim15 may act downstream of YlSch9. We found that Yl*sch9*Δ Yl*rim15*Δ cells exhibited a morphology close to that of Yl*rim15*Δ cells but not to Yl*sch9*Δ cells (Fig. 3A, top row). In addition, Yl*sch9*Δ Yl*rim15*Δ cells did not exhibit any radial filaments on YNBG agar, which is also close to Yl*rim15*Δ cells but not to Yl*sch9*Δ cells (Fig. 3A, second row). Moreover, TORC1 inhibitors failed to stimulate pseudohyphal outgrowth in Yl*sch9*Δ Yl*rim15*Δ cells (Fig. 3A, lower two rows). These results indicate that derepressed filamentation of Yl*sch9*Δ cells requires the presence of YlRim15. YlRim15 may be the target of YlSch9.

Unlike Yl*sch9*Δ cells, which did not exhibit a difference in morphology compared to wild-type cells in liquid YNBD medium, Yl*rim15*Δ cells exhibited reduced filamentous growth in this glucose medium (Fig. 3B). Yl*rim15*Δ cells were less elongated than wild-type cells as the average length of the mother cells was 11.3 ± 1.1 μm ($n = 160$), significantly shorter than that of wild-type cells (14.7 ± 1.4 μm, $n = 152$) ($P < 0.001$). Pseudohyphal formation appears to be normal (Yl*rim15*Δ cells: 7%, $n = 490$; Wild-type cells: 9%, $n = 460$). This result suggests that YlRim15 is necessary for efficient filamentation induced by glucose.

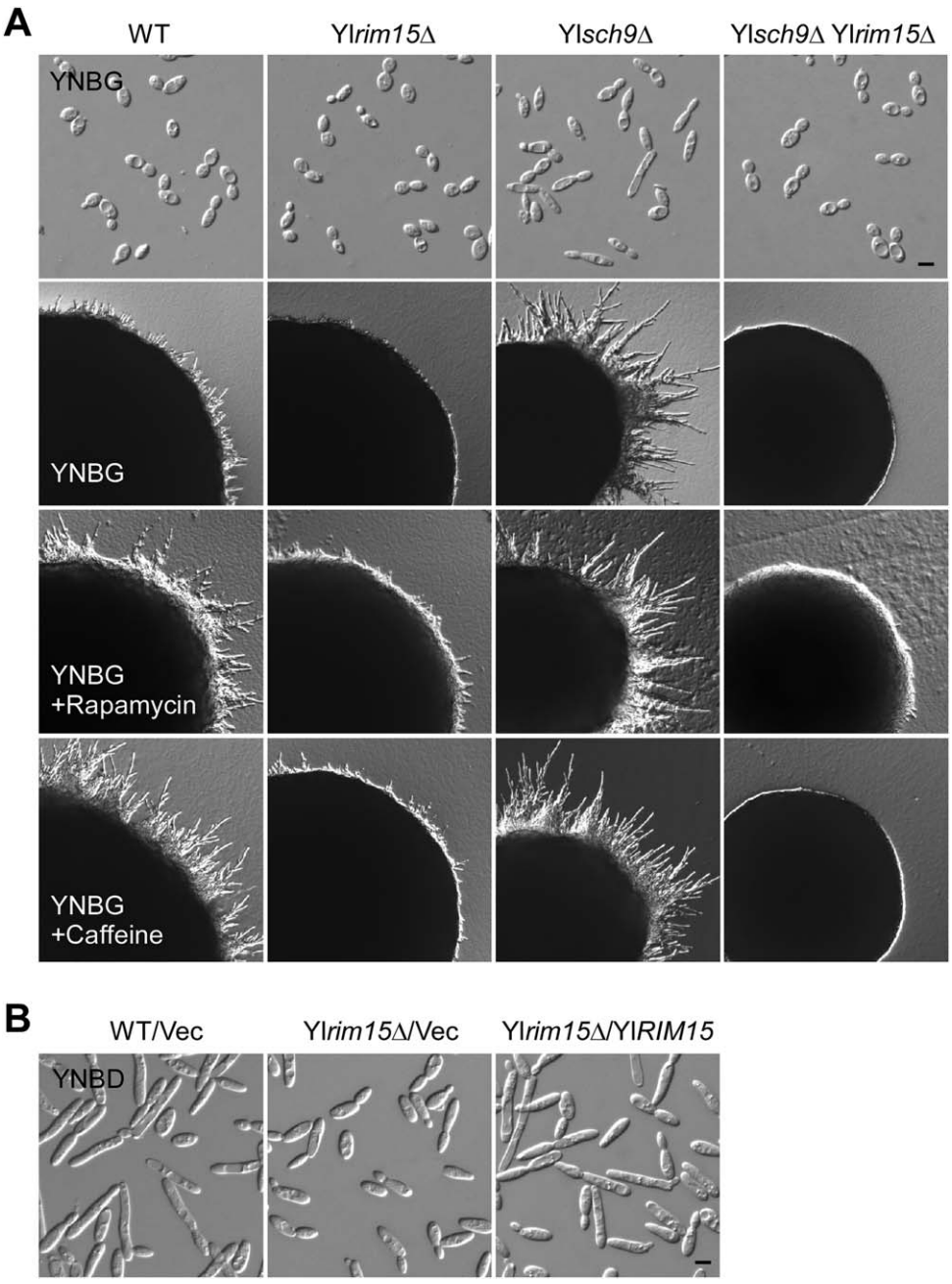

Fig. 3. YlRim15 may function downstream of the TORC1-YlSch9 signaling pathway in the repression of dimorphic transition.
A. Derepressed hyperfilamentation of TORC1-inhibited and Yl*sch9*Δ cells depends largely on YlRim15. Cells of strains carrying pINA445 were grown for 14 h in liquid YNBG medium or for 2 days on YNBG agar supplemented with 6.8 nM rapamycin or 1 mM caffeine.
B. Morphology of wild-type and Yl*rim15*Δ cells carrying pINA445 or pINA445-YlRIM15 in liquid YNBD medium supplemented with uracil.

Taken together, our results show that YlRim15 plays a positive role in dimorphic transition. YlRim15 may be a major target of the TORC1–Sch9 kinase casade, which may repress dimorphic transition via the repression of YlRim15 function.

YlSch9 represses YlRim15 by preventing its nuclear translocation

How does YlSch9 regulate YlRim15 in dimorphic transition? In *S. cerevisiae*, Sch9 inhibits Rim15's nuclear translocation to prevent Rim15 from activating downstream factors (Mirisola *et al*., 2014). We asked whether YlSch9 may regulate YlRim15 in a similar manner. We generated the Yl*RIM15-GFP* fusion construct and expressed it under the control of Yl*RIM15* promoter. Unfortunately, YlRim15-GFP fluorescence was too faint to detect. We then generated a *GFP*-Yl*RIM15* fusion construct and expressed it under control of the strong Yl*TEF1* promoter. This construct could complement the filamentation defect of Yl*rim15*Δ cells (data not shown). We observed that GFP-YlRim15 localized throughout the cytoplasm and the nucleus (indicated by DAPI staining) in wild-type cells grown in YNBG medium (Fig. 4A). In Yl*sch9*Δ cells and

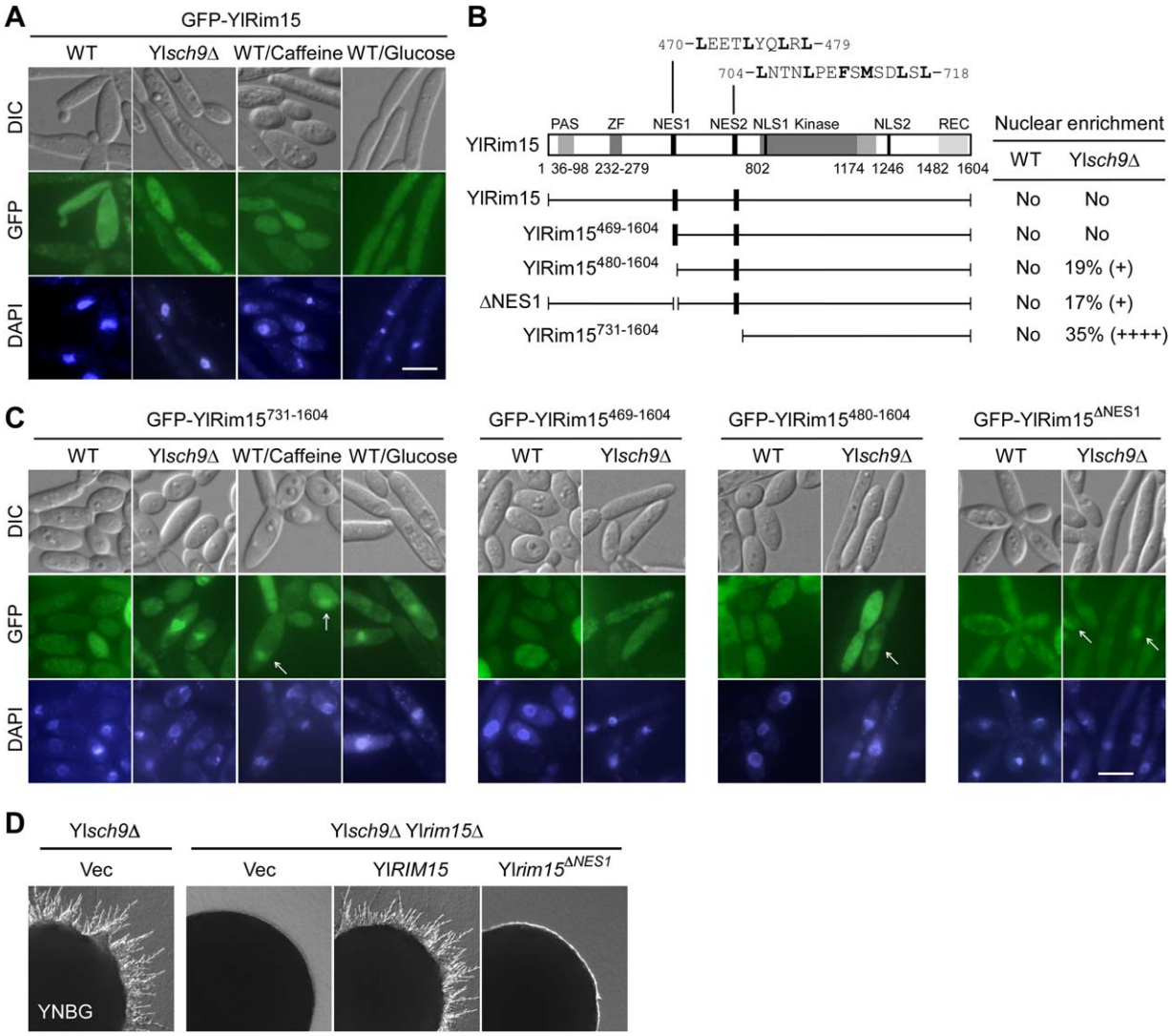

Fig. 4. TORC1–Sch9 inhibits the nuclear translocation of YlRim15.
A. Localization of GFP-YlRim15. Cells carrying pYL15-YlRIM15 were grown in liquid YNBG and YNBD media supplemented with uracil. Caffeine was added to final 1 mM when required. DNA was stained with DAPI.
B. Schematic representation of the domains of YlRim15 and the summary of nuclear localization of GFP-YlRim15 segments. The sequences of two NES motifs are shown. Percentages of cells that exhibited nuclear localization of GFP-YlRim15 segments are shown. The relative fluorescence intensities of nuclear GFP-YlRim15 segments are scored from strong (++++) to weak (+).
C. Localization of GFP-YlRim15 segments. Cells were grown in liquid YNBG medium supplemented with uracil except where noted.
D. Cells of Yl*sch9*Δ strain carrying pINA445 and cells of Yl*sch9*Δ Yl*rim15*Δ strain carrying pINA445, pINA445-YlRIM15 and pINA445-Ylrim15$^{\Delta NES1}$ were grown on YNBG agar medium supplemented with uracil. Colonies were photographed after 2 days. Scale bars, 5 μm.

wild-type cells treated with caffeine or grown in glucose, the localization of GFP-YlRim15 did not change. No particular enrichment in the nucleus could be seen (Fig. 4A). It seems that YlSch9 may not act by regulating the nucleocytoplasmic shuttling of YlRim15.

YlRim15 contains two potential NLS (nuclear localization sequence) motifs at the C-terminal region: NLS1 (821-KKATGEYFAIKTLKK-835) and NLS2 (1291-RKVPLHIPPHVRERRSRR-1308) (Fig. 4B). We found that, unlike full-length YlRim15, the YlRim15$^{731–1604}$ segment that contains the two NLS motifs showed a clear enrichment in the nucleus in 35% of Yl*sch9*Δ cells ($n = 68$) and 30% of caffeine-treated wild-type cells ($n = 71$). However, no nuclear enrichment could be seen in wild-type cells (Fig. 4C). This finding suggests that YlSch9 may play a role in the prevention of YlRim15 from entering the nucleus and thereby YlRim15 may be a downstream target of YlSch9. Interestingly, we found that YlRim15$^{731–1604}$ also exhibited clear nuclear enrichment in wild-type cells grown in YNBD medium (25%, $n = 123$) (Fig. 4C, see WT/Glucose. Relative fluorescence intensity: +++),

suggesting that YlSch9 may inhibit the nuclear translocation of YlRim15$^{731–1604}$ specifically in glycerol but not in glucose media.

Why full-length YlRim15 did not show nuclear enrichment in Yl*sch9*Δ cells? We reasoned that there might be NES (nuclear export signal) motifs that drive the export of YlRim15 out of the nucleus, preventing its nuclear accumulation. In support of this view, we identified two potential NES motifs at the N-terminal half of YlRim15 (Fig. 4B). We found that the YlRim15$^{469–1604}$ segment that carries both NES1 and NES2 did not show nuclear enrichment in Yl*sch9*Δ cells, just like full-length YlRim15 did (Fig. 4B and C). To determine which NES is required for the nuclear export, we examined the YlRim15$^{480–1604}$ segment that lacks only NES1 in comparison to YlRim15$^{469–1604}$. YlRim15$^{480–1604}$ exhibited nuclear enrichment in 19% of Yl*sch9*Δ cells ($n = 84$) (Fig. 4B and C), though its fluorescence intensity in the nucleus was markedly reduced compared to that of YlRim15$^{731–1604}$. Consistently, full-length YlRim15 lacking only NES1 also exhibited nuclear enrichment in 17% of Yl*sch9*Δ cells ($n = 92$) (Fig. 4B and C), indicating that NES1 is necessary for the nuclear export. The weaker nuclear fluorescence of YlRim15$^{480–1604}$ and YlRim15$^{\Delta NES1}$ compared to that of YlRim15$^{731–1604}$ suggests that NES2 may also play a role in the nuclear export. All these YlRim15 polypeptides were stably expressed as determined by immunoblotting with antibody against GFP (Fig. S5). These results indicate that nuclear export driven by NES1 and NES2 motifs may be responsible for the lack of nuclear enrichment of full-length YlRim15 in Yl*sch9*Δ and TORC1-inhibited cells. We observed that the expression of the Yl*rim15*$^{\Delta NES1}$ mutant expressed on low-copy plasmid under the control of Yl*RIM15* promoter failed to restore radial filament formation to Yl*sch9*Δ Yl*rim15*Δ cells on YNBG agar (Fig. 4D). This result suggests that it might be the dynamic nucleocytoplasmic shuttling rather than staying in the nucleus that is critical for YlRim15 function in dimorphic transition.

Together, our results suggest that YlRim15 is a downstream target of TORC1–Sch9 signaling pathway in the control of dimorphic transition. YlSch9 may repress YlRim15 function by preventing its nuclear translocation. The NES motifs play an important role in the nuclear export of YlRim15 and dynamic nucleocytoplasmic shuttling of YlRim15 is crucial for its function.

TORC1–Sch9 signaling down-regulates the expression of MHY1, a positive regulator of filamentous growth

The inhibition of YlRim15's nuclear translocation by TORC1–Sch9 signaling may block or reduce the expression of YlRim15-activated genes. We then examined the expression of genes that are known to be important for dimorphic transition and identified *MHY1* as a gene regulated by the TORC1–Sch9–Rim15 signaling pathway. *MHY1* encodes a zinc-finger transcription factor that contains two C_2H_2-type zinc finger motifs at its C-terminus. Previous studies have shown that *MHY1* plays a critical role in the regulation of dimorphic transition as the deletion of *MHY1* abolished filamentous growth while *MHY1* overexpression enhanced filamentous growth (Hurtado and Rachubinski, 1999; Li *et al.*, 2014). We found that *MHY1* overexpression also promoted strong hyphal growth in wild-type, Yl*rim15*Δ and Yl*sch9*Δ Yl*rim15*Δ cells grown in liquid glycerol medium (Fig. S5), suggesting that Mhy1 is an important regulator of dimorphic transition. We observed that the expression level of *MHY1* promoter-driven *lacZ* reporter (*MHY1-lacZ*) in wild-type cells was lower in glycerol medium than in glucose medium, the latter of which was 2.5- and 3-fold higher in liquid and solid media, respectively (Fig. 5). The differences were statistically significant ($P < 0.01$). Remarkably, *MHY1-lacZ* expression in Yl*sch9*Δ cells grown in glycerol medium increased substantially to the level comparable to those of wild-type cells and Yl*sch9*Δ cells grown in glucose medium (Fig. 5). This finding suggests that TORC1–Sch9 signaling down-regulates *MHY1* expression in glycerol medium but not in glucose medium. We found that the down-

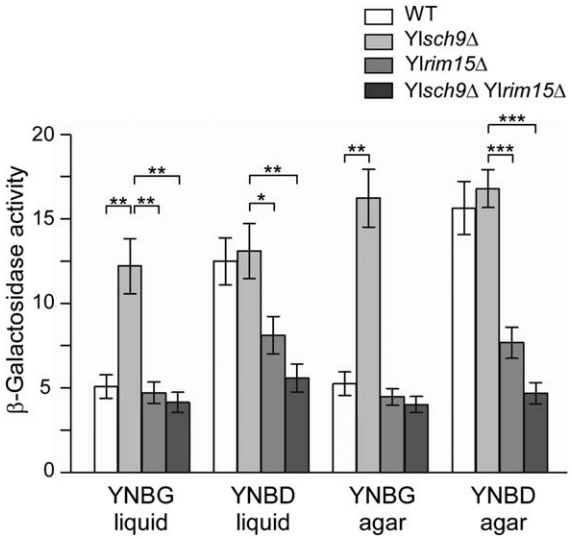

Fig. 5. TORC1–Sch9 signaling down-regulates the expression of *MHY1*, a positive regulator of filamentous growth.
Bar graph showing the expression levels of *MHY1-lacZ* in wild-type, Yl*sch9*Δ, Yl*rim15*Δ and Yl*sch9*Δ Yl*rim15*Δ strains. Cells were grown for 14 h in liquid YNBG and YNBD media supplemented with uracil or on YNBG or YNBD agar medium for 1 days. β-Galactosidase activity was measured. Error bars represent SD. Significant difference is indicated by $^*P < 0.02$, $^{**}P < 0.01$ and $^{***}P < 0.001$.

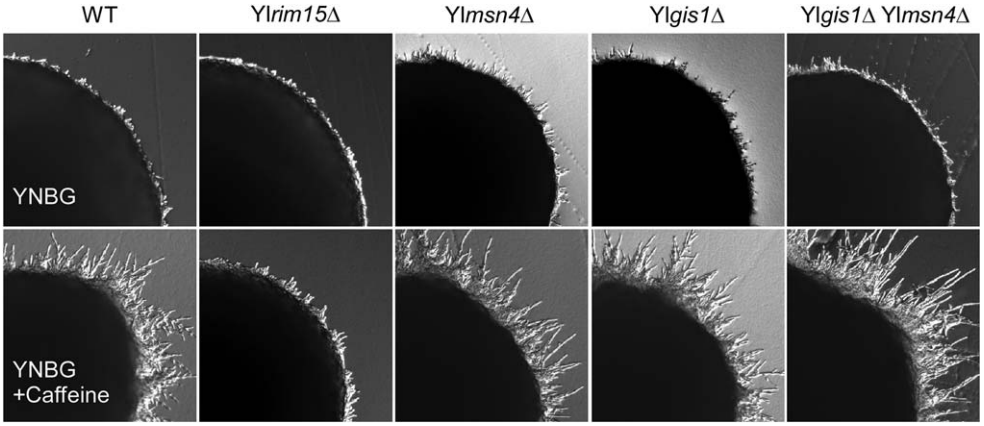

Fig. 6. YlRim15 may not function via YlMsn4 and YlGis1.
Cells of wild-type, Yl*rim15*Δ, Yl*msn4*Δ, Yl*gis1*Δ and Yl*msn4*Δ Yl*gis1*Δ strains carrying pINA445 were grown on YNBG agar medium supplemented with uracil and YNBG agar containing 1 mM caffeine. Colonies were photographed after 2 days.

regulation of *MHY1-lacZ* expression by TORC1–Sch9 depends on YlRim15 (Fig. 5), suggesting that *MHY1* is one of the target genes regulated by the TORC1–Sch9–Rim15 pathway.

YlRim15 may not function via YlMsn4 and YlGis1

In *S. cerevisiae*, activated Rim15 enters the nucleus and stimulates the transcription factors Msn2/4 and Gis1 to induce the expression of stress response genes (Martinez-Pastor *et al.*, 1996; Pedruzzi *et al.*, 2000). The *Y. lipolytica* genome encodes a single Msn2/4 homolog, YlMsn4 (YALI0C13750), and a Gis1 homolog, YlGis1 (YALI0F14487). To determine whether they may be the downstream targets of YlRim15 in dimorphic transition, we deleted Yl*MSN4* and Yl*GIS1*. We found that Yl*msn4*Δ, Yl*gis1*Δ and Yl*msn4*Δ Yl*gis1*Δ cells did not show any detectable defect in filamentous growth when grown in YNBD or hypha-inducing YNDC7 medium (data not shown). On YNBG agar, they formed colonies with short radial filaments as wild-type cells did (Fig. 6). TORC1 inhibition by caffeine induced further pseudohyphal outgrowth in these cells, just like in wild-type cells (Fig. 6). This result indicates that YlMsn4 and YlGis1 are dispensable for TORC1 inhibition-induced hyperfilamentation. Neither YlMsn4 nor YlGis1 may play a role in dimorphic transition. YlRim15 may function in dimorphic transition via other downstream factors.

Discussion

The oleaginous yeast *Y. lipolytica* grows in the yeast form in glycerol medium but in the filamentous form in glucose and fructose medium. What have kept the cells growing in the yeast form but not differentiating into the filamentous form in the presence of glycerol? In this study, we show that the evolutionarily conserved TORC1–Sch9 signaling pathway operates to repress dimorphic transition in response to glycerol abundance. The protein kinase YlRim15 is one of the major targets of the TORC1–Sch9 signaling pathway to repress dimorphic transition. Our results provide new insights into the regulation on dimorphic transition in fungi.

Role of TORC1 in the control of dimorphic transition

TORC1 regulates cell growth in response to nutrient availability from yeast to humans. TORC1 is known to repress stress response, the utilization of nonpreferred nutrients and autophagy under favorable conditions (Thomas and Hall, 1997; Schmelzle and Hall, 2000; Rohde *et al.*, 2001). In this study, we show that TORC1 also represses dimorphic transition under glycerol-rich condition in the yeast *Y. lipolytica*. This function is physiologically important since dimorphic transition is thought to be a foraging behavior (Gimeno *et al.*, 1992). There is no need to search for nutrients under nutrient-rich condition. TORC1 controls cellular processes via different downstream effectors. Our results show that TORC1 functions in the repression of dimorphic transition in *Y. lipolytica* via the protein kinase YlSch9, a homolog of mammalian p70 S6K. The repressive role of TORC1–Sch9 signaling on dimorphic transition was also found previously in *C. albicans* (Stichternoth *et al.*, 2011). In *S. cerevisiae*, although the role of TORC1 in dimorphic transition has not been investigated yet, TORC1–Sch9 signaling is also likely to repress this process since it was observed that the loss of Sch9 enhanced haploid invasive growth (Lorenz *et al.*, 2000). These observations in three evolutionarily divergent yeast species suggest that TORC1–Sch9 signaling may play a conserved role in the repression of dimorphic transition under favorable conditions in yeast.

*S. cerevisiae sch9*Δ mutant exhibited enhanced invasive growth when cultivated on YPD agar, which uses glucose as the carbon source (Lorenz *et al.*, 2000).

Surprisingly, we observed that *Y. lipolytica* Yl*sch9*Δ cells did not display enhanced filamentation on synthetic YNBD medium, which also uses glucose as the carbon source. The repressive role of the TORC1–Sch9 pathway is instead apparent on synthetic medium with glycerol as the carbon source. Similarly, studies in *C. albicans* showed that TORC1–Sch9 signaling represses dimorphic transition only under hypoxia at high CO_2 levels (Stichternoth *et al*., 2011), but not on YPD or Spider medium (Liu *et al*., 2010). These observations suggest that the TORC1–Sch9 pathway may have diverged significantly and become specialized in the sensing of different nutrient signals in three yeast species. TORC1 plays an evolutionarily conserved role in sensing nitrogen sources, amino acids and, possibly, carbon sources (Rohde *et al*., 2001). In *Y. lipolytica*, the TORC1–Sch9 pathway may integrate glycerol sensing to the repression of dimorphic transition. To our knowledge, this is the first report that the yeast TORC1–Sch9 pathway may sense glycerol, a carbon source.

Why does the TORC1–Sch9 pathway in *Y. lipolytica* repress dimorphic transition in the presence of glycerol but not glucose like *S. cerevisiae* does? The difference may have originated from their different life styles. *S. cerevisiae* lives in the glucose-rich environment (grape skin) and is known to be glucophilic. Its metabolism is highly adapted to the utilization of glucose. *S. cerevisiae* has 18 hexose transporters for the uptake of glucose whereas *Y. lipolytica* has just one (plus three high-affinity glucose transporters) (Wieczorke *et al*., 1999; Palma *et al*., 2007). In contrast, *Y. lipolytica* lives in lipid- and protein-rich environment (cheese and sausages) (Groenewald *et al*., 2014). It secretes extracellular lipases and proteases to break down these substrates. Glycerol could be obtained from triacylglycerols by the action of lipases. In comparison to glucose, glycerol is a preferred carbon source for *Y. lipolytica* as cells exhibited more robust growth on glycerol than on glucose (Mori *et al*., 2013). *Y. lipolytica* has six glycerol transporters to mediate the uptake of glycerol whereas *S. cerevisiae* has just one (Palma *et al*., 2007). Thus, the presence of glycerol may signal that the carbon source is rich and favorable and there is no need to differentiate into filaments (to forage for nutrients).

TORC1 activity in the cells is thought to be high under nutrient-rich condition and low under starvation. It is known that nitrogen starvation could induce filamentous growth in several yeast species. Interestingly, the low TORC1 activity is required for filamentous growth as TORC1 inhibition by rapamycin blocked filamentation in divergent yeast species *S. cerevisiae*, *C. albicans*, *Candida lustaniae* and *Cryptococcus neoformans* under nitrogen starvation (Cutler *et al*., 2001). TORC1's function in this process is thought to be mediated by the TORC1–Tap42–Sit4 pathway. TORC1 phosphorylates Tap42, a regulatory subunit of the protein phosphatase PP2A and Sit4. Phosphorylated Tap42 then binds to Sit4 and regulates translation and the nitrogen catabolite repression (NCR) transcriptional response (Di Como and Arndt, 1996; Beck and Hall, 1999; Bertram *et al*., 2000). These results suggest that TORC1 may elicit both positive and negative regulation on dimorphic transition depending on nutrient abundance or limitation via different downstream effectors. The TORC1–Sch9 pathway may operate to sense high levels of nutrients and prevent filamentous growth when nutrients are abundant. The TORC1–Tap42–Sit4 pathway, however, may be important for cell growth under both nutrient-rich and nutrient-poor conditions. Particularly, under nutrient-poor condition, the low TORC1 activity may be essential for the expression of genes important for filamentous growth.

Effectors downstream of the TORC1–Sch9 pathway in the repression of dimorphic transition

In *S. cerevisiae*, TORC1–Sch9 signaling regulates life span, calorie restriction-dependent stress resistance and the expression of genes required for survival in G_0 via the protein kinase Rim15 (Pedruzzi *et al*., 2003; Wei *et al*., 2008). TORC1–Sch9 signaling prevents the nuclear translocation of Rim15 (Pedruzzi *et al*., 2003). Sch9 phosphorylates the Ser 1061 residue of Rim15 and this phosphorylation causes the cytoplasmic retention of Rim15 (Wanke *et al*., 2008). In this study, we show that the repressive function of YlSch9 on dimorphic transition in *Y. lipolytica* also depends largely on YlRim15. Similar to *S. cerevisiae* Sch9, YlSch9 also prevents the nuclear translocation of YlRim15 in glycerol medium, suggesting that the TORC1–Sch9–Rim15 signaling pathway is conserved compared to that of *S. cerevisiae*, at least down to the level of Rim15. However, certain differences still exist. First, YlRim15 did not exhibit a strong enrichment in the nucleus in Yl*sch9*Δ cells as *S. cerevisiae* Rim15 did in *sch9*Δ cells. Our results suggest that the dynamic nucleocytoplasmic shuttling of YlRim15 rather than the accumulation of YlRim15 in the nucleus may be required for the action of YlRim15. Second, *S. cerevisiae* Rim15 controls the expression of stress responsive genes and diauxic shift genes via the transcription factors Msn2/4 and Gis1, respectively (Cameroni *et al*., 2004; Swinnen *et al*., 2006). We observed that the *Y. lipolytica* homologs of Msn2/4 and Gis1 are not required for YlRim15's function in dimorphic transition. YlRim15 may regulate this process via other yet unknown effectors.

In light of these observations, we proposed a model to explain how TORC1–Sch9 signaling may repress dimorphic transition. When glycerol is abundant, TORC1 activity is high. YlSch9 is activated by TORC1

and Pkh1 (yeast homolog of mammalian PDK1) via phosphorylation. Activated YlSch9 inhibited the nuclear translocation of YlRim15 presumably via the phosphorylation of YlRim15. YlRim15 is then kept in the cytoplasm, which prevents the activation of transcription factors regulated by YlRim15 and blocks the expression of genes involved in filamentous growth (FG) (Fig. 7A). In contrast, glycerol depletion would cause a dramatic reduction of TORC1 activity in the cells, which would render YlSch9 no longer active. YlRim15 is thereby released from YlSch9 inhibition. As a result, YlRim15 would enter the nucleus and activate transcription factors responsible for the expression of genes involved in filamentous growth, leading to filamentation (Fig. 7B). *MHY1* appears to be one of these genes regulated by the TORC1–Sch9–Rim15 signaling pathway. Mhy1 is most similar to *S. cerevisiae* Yer130c and *C. albicans* Mnl1. Mnl1 is reported to regulate weak acid stress responses (Ramsdale *et al.*, 2008), while the function of Yer130c is not clear.

This model could not explain the behavior of cells in the presence of glucose. TORC1 activity is presumably to be high in the cells cultivated in glucose medium. However, the cells undergo filamentous growth unlike those cultivated in glycerol medium, which stay in the yeast form. Deletion of Yl*SCH9* did not promote further hyperfilamentation, suggesting that TORC1–Sch9 signaling no longer represses filamentation. In support of this view, we observed that YlRim15$^{731–1604}$ displayed a nuclear enrichment in cells grown in glucose medium (Fig. 4C, see WT/glucose), suggesting that YlRim15 is released from the inhibition by YlSch9. It is currently not clear why TORC1–Sch9 no longer inhibits YlRim15 in glucose medium.

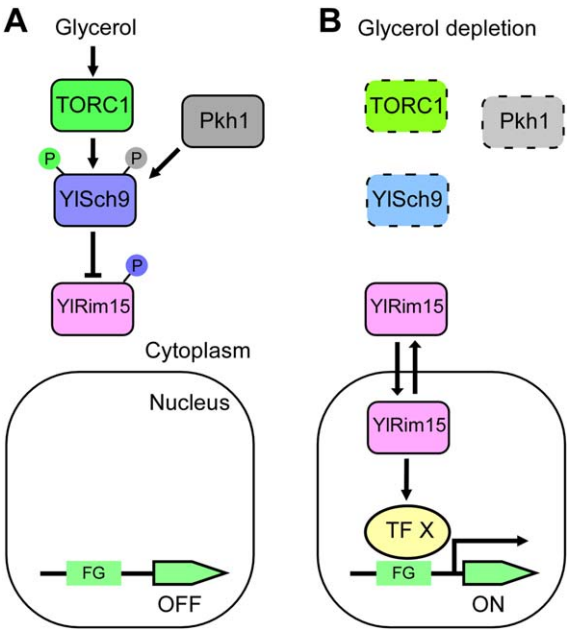

Fig. 7. A model on the repression of dimorphic transition by TORC1–Sch9–Rim15 signaling in response to glycerol.
TF X represents transcription factors regulated by YlRim15. FG stands for genes implicated in filamentous growth.

At this time, it is not known whether YlSch9 may phosphorylate YlRim15 and if so, the phosphorylation of which residue is important for YlRim15 inactivation. The region in *S. cerevisiae* Rim15 that contains the Sch9-phosphorylated site, Ser 1061, is not conserved in YlRim15. This has posted a challenge to investigate the mechanism by which YlSch9 regulates YlRim15.

C. albicans CaSch9 also negatively regulates filamentation but specifically under hypoxia at high CO_2 levels (Stichternoth *et al.*, 2011), a condition that resembles the environment in the human gut where *C. albicans* normally lives. Transcriptomal analysis of the Ca*sch9* mutant showed that the transcription levels of 310 genes were altered at least 2-fold compared to the wild-type strain. Surprisingly, CaRim15 does not function downstream of CaSch9 in the regulation of dimorphic transition under this growth condition (Stichternoth *et al.*, 2011). It is possible that the downstream effector of the TORC1–Sch9 pathway may have diverged in *C. albicans* or the TORC1–Sch9 may still regulate dimorphic transition via Rim15 but specifically under other growth conditions.

While TORC1–Sch9–Rim15 signaling is important for the repression of dimorphic transition in *Y. lipolytica*, YlSch9 may also have other targets apart from YlRim15. We observed that pseudohyphal outgrowth of Yl*rim15*Δ cells grown on YNBG agar can be slightly stimulated by rapamycin or caffeine (Fig. 3A). This result supports this view. Future investigations are needed to identify additional targets of the TORC1–Sch9 pathway. In this study, we also observed that *Y. lipolytica* cells grown in liquid sodium oleate medium were in the oval-shaped yeast form, just like the cells grown in glycerol medium, suggesting that dimorphic transition is also repressed in liquid sodium oleate medium. However, unlike in glycerol medium, we found that Yl*sch9*Δ cells grown in liquid sodium oleate medium were still in the yeast form (Fig. S2B). This observation suggests that YlSch9 is dispensable for the repression of dimorphic transition by sodium oleate. It is likely that signaling pathways other than TORC1–Sch9 may exist in *Y. lipolytica* for the repression of dimorphic transition in sodium oleate medium.

Experimental Procedures

Strains, media and genetic methods

Y. lipolytica strain PO1a (*MatA leu2-270 ura3-302*) was kindly provided by Dr Claude Gaillardin (INRA,

Thiverval-Grignon, France). *Escherichia coli* strain DH5α was used for plasmid amplification. *Y. lipolytica* strains were routinely grown at 30°C in YNBD medium (0.67% yeast nitrogen base without amino acid, 2% glucose) or YNBG medium (0.67% yeast nitrogen base without amino acid, 1% glycerol) supplemented with 80 mg/l of leucine, 20 mg/l of uracil or both when required. For solid media, agar was added to 2%. Fructose, peptone, sodium lactate, sodium citrate or sodium oleate were added to the YNB medium at the final concentration of 1%. YNDC7 medium (0.67% yeast nitrogen base without amino acid, 2.94% trisodium citrate dehydrate, 1% glucose, pH 7.0) was used for hyphal growth. The lithium acetate method was used to transform *Y. lipolytica* cells (Zhao *et al*., 2013).

Gene deletion

Oligonucleotides used in this study are listed in Table S1. Yl*SCH9* was deleted in strain PO1a by homologous recombination. Briefly, a ~1.0-kb sequence upstream of the Yl*SCH9* open reading frame (ORF) (YlSCH9P) and a ~1.0-kb sequence downstream of ORF (YlSCH9T) were amplified by PCR from genomic DNA using YlSCH9-PF/YlSCH9-PR and YlSCH9-TF/YlSCH9-TR primer pairs, respectively. YlSCH9P and YlSCH9T were then inserted into the flanking sites of *loxR*-Yl*URA3*-*loxP* in pYL8 (Zhao *et al*., 2013). The resulting Yl*SCH9P*-*loxR*-Yl*URA3*-*loxP*-Yl*SCH9T* deletion cassette was used to transform strain PO1a. Ura^+ transformants were examined by PCR to identify the clones that bear the correct replacement of Yl*SCH9*. At least two independent correct clones were obtained. The Yl*URA3* marker was later excised by Cre-mediated site-specific DNA recombination between *loxR* and *loxP* sites (Zhao *et al*., 2013), yielding YLX500 (Yl*sch9*Δ::*loxR/P*). Yl*RIM15*, Yl*MSN4* and Yl*GIS1* were deleted in strain PO1a in a similar manner, yielding YLX501 (Yl*rim15*Δ::*loxR/P*), YLX503 (Yl*msn4*Δ::*loxR/P*) and YLX504 (Yl*gis1*Δ::*loxR/P*). Yl*SCH9* was deleted in strain YLX501, yielding YLX502 (Yl*sch9*Δ::*loxR/P* Yl*rim15*Δ::*loxR/P*). Yl*GIS1* was deleted in strain YLX503, yielding YLX505 (Yl*msn4*Δ::*loxR/P* Yl*gis1*Δ::*loxR/P*).

Plasmid construction

The 3.5-kb Yl*SCH9* gene containing 1011-bp promoter, 2052-bp ORF and 399-bp 3′-UTR was amplified by PCR using primers YlSCH9-1F and YlSCH9-1R and inserted into *Sph*I- and *Hin*dIII-digested pINA445 (*CEN*, Yl*LEU2*) to generate pINA445-YlSCH9. Yl$sch9^{T470A}$ and Yl$sch9^{T634A}$ mutants were generated from pINA445-YlSCH9 by overlapping PCR using primer pairs YlSCH9-T470F/YlSCH9-T470R and YlSCH9-T634F/YlSCH9-T634R, respectively. Yl*SCH9*, Yl$sch9^{T470A}$ and Yl$sch9^{T634A}$ mutants carrying 932-bp Yl*SCH9* promoter were PCR-amplified using primers YlSCH9-2F and YlSCH9-2R and inserted into *Bam*HI- and *Hin*dIII-digested pYL14 (pINA445 backbone, Yl*LEU2*, *GFP*-T_{YlURA3}) (Zhao *et al*., 2013) to generate Yl*SCH9-GFP* fusion constructs. The 6.3-kb Yl*RIM15* gene containing 1072-bp promoter, 4815-bp ORF and 390-bp 3′-UTR was amplified by PCR using primers YlRIM15-PF and YlRIM15-1R and inserted into *Bam*HI-digested pINA445, yielding pINA445-YlRIM15. The Yl$rim15^{\Delta NES1}$ mutant was constructed from pINA445-YlRIM15 by overlapping PCR using primers YlRIM15-NESF and YlRIM15-NESR. To examine the subcellular localization of YlRim15 and YlRim15 segments, DNA fragments containing Yl*RIM15* ORF (4.8 kb), Yl*RIM15* segments or Yl$rim15^{\Delta NES1}$ carrying 390-bp 3′-UTR were amplified from pINA445-YlRIM15 or pINA445-Ylrim$15^{\Delta NES1}$ by PCR and inserted into *Bam*HI- and *Kpn*I-digested pYL15 (pINA445 backbone, Yl*LEU2*, P_{YlTEF1}-*GFP*) (Li *et al*., 2014). GFP was fused in frame to the N-terminus of YlRim15. To overexpress Yl*SCH9*, Yl*SCH9* ORF was amplified by PCR using primers YlSCH9-OF and YlSCH9-1R and inserted into *Xba*I- and *Hin*dIII-digested pYL13 (pINA445 backbone, Yl*LEU2*, P_{YlTEF1}) (Zhao *et al*., 2013). To generate the *MHY1-lacZ* reporter, 3.7 kb promoter of *MHY1* plus the ATG start codon was PCR-amplified from genomic DNA using primers MHY1-3.7KF and MHY1-HBR, digested with *Hin*dIII and *Sal*I and ligated into pINA445-lacZ (Zhao *et al*., 2013), yielding pINA445-MHY1-lacZ. pYL13-MHY1 was constructed similar to pYL13-YlSCH9.

β-Galactosidase assay

β-Galactosidase activity in the cells was determined by crude cell extract assay and normalized by protein concentration in the cell lysate as reported previously (Zhao *et al*., 2013).

Microscopy

An Olympus BX51 microscope (Tokyo, Japan) and a Retiga 2000R CCD camera (QImaging Corporation, Canada) were used to visualize cell morphology and GFP by differential interference contrast (DIC) and fluorescent microscopy. For DNA staining, yeast cells were stained with 4′,6′-diamidino-2-phenylindole (DAPI) (Sigma-Aldrich, St Louis, MO) at 1 μg/ml. The images were acquired using QCapture Suite (QImaging Corporation, Surrey, BC, Canada).

Acknowledgements

We thank Drs Claude Gaillardin, Jean-Marie Beckerich, Jean-Marc Nicaud and Richard Rachubinski for kindly providing yeast strains and plasmids. This work was supported by the National Natural Science Foundation of China (grant numbers 31370124 and 31570076) and National Infrastructure of Natural Resources for Science and Technology Program of China (grant number NIMR-2017-8).

References

Barth, G., and Gaillardin, C. (1997) Physiology and genetics of the dimorphic fungus *Yarrowia lipolytica*. *FEMS Microbiol Rev* **19**: 219–237.

Beck, T., and Hall, M.N. (1999) The TOR signalling pathway controls nuclear localization of nutrient-regulated transcription factors. *Nature* **402**: 689–692.

Berman, J., and Sudbery, P.E. (2002) *Candida albicans*: a molecular revolution built on lessons from budding yeast. *Nat Rev Genet* **3**: 918–930.

Bertram, P.G., Choi, J.H., Carvalho, J., Ai, W., Zeng, C., Chan, T.F., and Zheng, X.F. (2000) Tripartite regulation of Gln3p by TOR, Ure2p, and phosphatases. *J Biol Chem* **275**: 35727–35733.

Cameroni, E., Hulo, N., Roosen, J., Winderickx, J., and De Virgilio, C. (2004) The novel yeast PAS kinase Rim 15 orchestrates G_0-associated antioxidant defense mechanisms. *Cell Cycle* **3**: 462–468.

Csank, C., Schröppel, K., Leberer, E., Harcus, D., Mohamed, O., Meloche, S., *et al*. (1998) Roles of the *Candida albicans* mitogen-activated protein kinase homolog, Cek1p, in hyphal development and systemic candidiasis. *Infect Immun* **66**: 2713–2721.

Cutler, N.S., Pan, X., Heitman, J., and Cardenas, M.E. (2001) The TOR signal transduction cascade controls cellular differentiation in response to nutrients. *Mol Biol Cell* **12**: 4103–4113.

deHart, A.K., Schnell, J.D., Allen, D.A., Tsai, J.Y., and Hicke, L. (2003) Receptor internalization in yeast requires the Tor2-Rho1 signaling pathway. *Mol Biol Cell* **14**: 4676–4684.

Di Como, C.J., and Arndt, K.T. (1996) Nutrients, via the Tor proteins, stimulate the association of Tap42 with type 2A phosphatases. *Genes Dev* **10**: 1904–1916.

Dujon, B., Sherman, D., Fischer, G., Durrens, P., Casaregola, S., Lafontaine, I., and Al, e. (2004) Genome evolution in yeasts. *Nature* **430**: 35–44.

Fabrizio, P., Pozza, F., Pletcher, S.D., Gendron, C.M., and Longo, V.D. (2001) Regulation of longevity and stress resistance by Sch9 in yeast. *Science* **292**: 288–290.

Gimeno, C.J., Ljungdahl, P.O., Styles, C.A., and Fink, G.R. (1992) Unipolar cell divisions in the yeast *S. cerevisiae* lead to filamentous growth: regulation by starvation and *RAS*. *Cell* **68**: 1077–1090.

Groenewald, M., Boekhout, T., Neuveglise, C., Gaillardin, C., Van Dijck, P.W.M., and Wyss, M. (2014) *Yarrowia lipolytica*: safety assessment of an oleaginous yeast with a great industrial potential. *Crit Rev Microbiol* **40**: 187–206.

Hurtado, C.A., and Rachubinski, R.A. (1999) *MHY1* encodes a C_2H_2-type zinc finger protein that promotes dimorphic transition in the yeast *Yarrowia lipolytica*. *J Bacteriol* **181**: 3051–3057.

Isotani, S., Hara, K., Tokunaga, C., Inoue, H., Avruch, J., and Yonezawa, K. (1999) Immunopurified mammalian target of rapamycin phosphorylates and activates p70 S6 kinase alpha *in vitro*. *J Biol Chem* **274**: 34493–34498.

Kadosh, D. (2013) Shaping up for battle: morphological control mechanisms in human fungal pathogens. *PLoS Pathog* **9**: e1003795.

Kaeberlein, M., Powers, RWr., Steffen, K.K., Westman, E.A., Hu, D., Dang, N., *et al*. (2005) Regulation of yeast replicative life span by TOR and Sch9 in response to nutrients. *Science* **310**: 1193–1196.

Leberer, E., Harcus, D., Dignard, D., Johnson, L., Ushinsky, S., Thomas, D.Y., and Schroppel, K. (2001) Ras links cellular morphogenesis to virulence by regulation of the MAP kinase and cAMP signaling pathways in the pathogenic fungus *Candida albicans*. *Mol Microbiol* **42**: 673–687.

Lengeler, K.B., Davidson, R.C., D'souza, C., Harashima, T., Shen, W.C., Wang, P., *et al*. (2000) Signal transduction cascades regulating fungal development and virulence. *Microbiol Mol Biol Rev* **64**: 746–785.

Li, M., Li, Y.Q., Zhao, X., and Gao, X.D. (2014) Roles of the three Ras proteins in the regulation of dimorphic transition in the yeast *Yarrowia lipolytica*. *FEMS Yeast Res* **14**: 451–463.

Liu, W., Zhao, J., Li, X., Li, Y., and Jiang, L. (2010) The protein kinase CaSch9p is required for the cell growth, filamentation and virulence in the human fungal pathogen *Candida albicans*. *FEMS Yeast Res* **10**: 462–470.

Loewith, R., Jacinto, E., Wullschleger, S., Lorberg, A., Crespo, J.L., Bonenfant, D., *et al*. (2002) Two TOR complexes, only one of which is rapamycin sensitive, have distinct roles in cell growth control. *Mol Cell* **10**: 457–468.

López-Berges, M.S., Rispail, N., Prados-Rosales, R.C., and Di Pietro, A. (2010) A nitrogen response pathway regulates virulence functions in *Fusarium oxysporum* via the protein kinase TOR and the bZIP protein MeaB. *Plant Cell* **22**: 2459–2275.

Lorenz, M.C., Pan, X., Harashima, T., Cardenas, M.E., Xue, Y., Hirsch, J.P., and Heitman, J. (2000) The G protein-coupled receptor Gpr1 is a nutrient sensor that regulates pseudohyphal differentiation in *Saccharomyces cerevisiae*. *Genetics* **154**: 609–622.

Lu, Y., Su, C., and Liu, H. (2014) *Candida albicans* hyphal initiation and elongation. *Trends Microbiol* **22**: 707–714.

Martinez-Pastor, M.T., Marchler, G., Schuller, C., Marchler-Bauer, A., Ruis, H., and Estruch, F. (1996) The *Saccharomyces cerevisiae* zinc finger proteins Msn2p and Msn4p are required for transcriptional induction through the stress response element (STRE). *EMBO J* **15**: 2227–2235.

Matsuo, T., Otsubo, Y., Urano, J., Tamanoi, F., and Yamamoto, M. (2007) Loss of the TOR kinase Tor2 mimics nitrogen starvation and activates the sexual development pathway in fission yeast. *Mol Cell Biol* **27**: 3154–3164.

Mirisola, M.G., Taormina, G., Fabrizio, P., Wei, M., Hu, J., and Longo, V.D. (2014) Serine- and threonine/valine-dependent activation of PDK and Tor orthologs converge on Sch9 to promote aging. *PLoS Genet* **10**: e1004113.

Mora, A., Komander, D., van Aalten, D.M., and Alessi, D.R. (2004) PDK1, the master regulator of AGC kinase signal transduction. *Semin Cell Dev Biol* **15**: 161–170.

Mori, K., Iwama, R., Kobayashi, S., Horiuchi, H., Fukuda, R., and Ohta, A. (2013) Transcriptional repression by glycerol of genes involved in the assimilation of *n*-alkanes and fatty acids in yeast *Yarrowia lipolytica*. *FEMS Yeast Res* **13**: 233–240.

Mosch, H.U., Roberts, R.L., and Fink, G.R. (1996) Ras2 signals via the Cdc42/Ste20/mitogen-activated protein kinase module to induce filamentous growth in *Saccharomyces cerevisiae*. *Proc Natl Acad Sci USA* **93**: 5352–5356.

Palecek, S.P., Parikh, A.S., and Kron, S.J. (2002) Sensing, signaling and integrating physical processes during *Saccharomyces cerevisiae* invasive and filamentous growth. *Microbiology* **148**: 893–907.

Palma, M., Goffeau, A., Spencer-Martins, I., and Baret, P.V. (2007) A phylogenetic analysis of the sugar porters in hemiascomycetous yeasts. *J Mol Microbiol Biotechnol* **12**: 241–248.

Pedruzzi, I., Burckert, N., Egger, P., and De Virgilio, C. (2000) *Saccharomyces cerevisiae* Ras/cAMP pathway controls post-diauxic shift element-dependent transcription through the zinc finger protein Gis1. *EMBO J* **19**: 2569–2579.

Pedruzzi, I., Dubouloz, F., Cameroni, E., Wanke, V., Roosen, J., Winderickx, J., and De Virgilio, C. (2003) TOR and PKA signaling pathways converge on the protein kinase Rim15 to control entry into G_0. *Mol Cell* **12**: 1607–1613.

Ramsdale, M., Selway, L., Stead, D., Walker, J., Yin, Z., Nicholls, S.M., *et al*. (2008) *MNL1* regulates weak acid-induced stress responses of the fungal pathogen *Candida albicans*. *Mol Biol Cell* **19**: 4393–4403.

Reinke, A., Chen, J.C., Aronova, S., and Powers, T. (2006) Caffeine targets TOR complex I and provides evidence for a regulatory link between the FRB and kinase domains of Tor1p. *J Biol Chem* **281**: 31616–31626.

Robertson, L.S., and Fink, G.R. (1998) The three yeast A kinases have specific signaling functions in pseudohyphal growth. *Proc Natl Acad Sci USA* **95**: 13783–13787.

Rohde, J., Heitman, J., and Cardenas, M.E. (2001) The TOR kinases link nutrient sensing to cell growth. *J Biol Chem* **276**: 9583–9586.

Roosen, J., Engelen, K., Marchal, K., Mathys, J., Griffioen, G., Cameroni, E., *et al*. (2005) PKA and Sch9 control a molecular switch important for the proper adaptation to nutrient availability. *Mol Microbiol* **55**: 862–880.

Ruiz-Herrera, J., and Sentandreu, R. (2002) Different effectors of dimorphism in *Yarrowia lipolytica*. *Arch Microbiol* **178**: 477–483.

Sarbassov, D.D., Guertin, D.A., Ali, S.M., and Sabatini, D.M. (2005) Phosphorylation and regulation of Akt/PKB by the rictor-mTOR complex. *Science* **307**: 1098–1101.

Sarkaria, J.N., Busby, E.C., Tibbetts, R.S., Roos, P., Taya, Y., Karnitz, L.M., and Abraham, R.T. (1999) Inhibition of ATM and ATR kinase activities by the radiosensitizing agent, caffeine. *Cancer Res* **59**: 4375–4382.

Schmelzle, T., and Hall, M.N. (2000) TOR, a central controller of cell growth. *Cell* **103**: 253–262.

Schmidt, A., Kunz, J., and Hall, M.N. (1996) TOR2 is required for organization of the actin cytoskeleton in yeast. *Proc Natl Acad Sci USA* **93**: 13780–13785.

Stichternoth, C., Fraund, A., Setiadi, E., Giasson, L., Vecchiarelli, A., and Ernst, J.F. (2011) Sch9 kinase integrates hypoxia and CO_2 sensing to suppress hyphal morphogenesis in *Candida albicans*. *Eukaryot Cell* **10**: 502–511.

Swinnen, E., Wanke, V., Roosen, J., Smets, B., Dubouloz, F., Pedruzzi, I., *et al*. (2006) Rim15 and the crossroads of nutrient signalling pathways in *Saccharomyces cerevisiae*. *Cell Div* **1**: 3.

Thomas, G., and Hall, M.N. (1997) TOR signalling and control of cell growth. *Curr Opin Cell Biol* **9**: 782–787.

Urban, J., Soulard, A., Huber, A., Lippman, S., Mukhopadhyay, D., Deloche, O., *et al*. (2007) Sch9 is a major target of TORC1 in *Saccharomyces cerevisiae*. *Mol Cell* **26**: 663–674.

Varshney, N., Schaekel, A., Singha, R., Chakraborty, T., van Wijlick, L., Ernst, J.F., and Sanyal, K. (2015) A surprising role for the Sch9 protein kinase in chromosome segregation in *Candida albicans*. *Genetics* **199**: 671–674.

Wanke, V., Cameroni, E., Uotila, A., Piccolis, M., Urban, J., Loewith, R., and De Virgilio, C. (2008) Caffeine extends yeast lifespan by targeting TORC1. *Mol Microbiol* **69**: 277–285.

Wei, M., Fabrizio, P., Hu, J., Ge, H., Cheng, C., Li, L., and Longo, V.D. (2008) Life span extension by calorie restriction depends on Rim15 and transcription factors downstream of Ras/PKA, Tor, and Sch9. *PLoS Genet* **4**: e13.

Wieczorke, R., Krampe, S., Weierstall, T., Freidel, K., Hollenberg, C.P., and Boles, E. (1999) Concurrent knock-out of at least 20 transporter genes is required to block uptake of hexoses in *Saccharomyces cerevisiae*. *FEBS Lett* **464**: 123–128.

Wullschleger, S., Loewith, R., and Hall, M.N. (2006) TOR signaling in growth and metabolism. *Cell* **124**: 471–484.

Zhao, X.F., Li, M., Li, Y.Q., Chen, X.D., and Gao, X.D. (2013) The TEA/ATTS transcription factor YlTec1p represses the yeast-to-hypha transition in the dimorphic yeast *Yarrowia lipolytica*. *FEMS Yeast Res* **13**: 50–61.

Zinjarde, S.S., Kale, B.V., Vishwasrao, P.V., and Kumar, A.R. (2008) Morphogenetic behavior of tropical marine yeast *Yarrowia lipolytica* in response to hydrophobic substrates. *J Microbiol Biotechnol* **18**: 1522–1528.

Supporting information

Additional supporting information may be found in the online version of this article at the publisher's web-site.